

Casimir force on a thin slab: The influence of surrounding media and the role of surface polaritons

Z. Lenac

Department of Physics, University of Rijeka, 51000 Rijeka, Croatia

M. S. Tomaš

Institute Rudjer Bošković, P.O. Box 180, 10002 Zagreb, Croatia

(Received 2 June 2008; revised manuscript received 20 July 2008; published 25 August 2008)

We consider the Casimir force on a metallic slab with the thickness in the nanometer range, bounded by different dielectric media. In such systems the force is large ($\sim 10^6$ N/m²) and, depending on the selected configuration, it can be squeezing or relaxing. The mode analysis, performed numerically as well as analytically under the assumption of inert bounding media, indicates that the force on a thin metallic slab is, in many situations, predominantly due to the surface polariton (SP) modes of the system (an obvious exception is the configuration with the slab sandwiched between two highly reflecting plates). Thus, the sign and the magnitude of the Casimir force are typically determined by competing contributions from the two SP modes existing in the model adopted, and are controllable by properly designing the system parameters. The same conclusion holds for a more complex description of polar dielectric media, assuming that the characteristic frequencies of polar modes in dielectrics are much smaller than the characteristic plasma frequency of a metallic slab.

DOI: [10.1103/PhysRevA.78.023834](https://doi.org/10.1103/PhysRevA.78.023834)

PACS number(s): 42.50.Ct, 12.20.-m, 73.20.Mf

I. INTRODUCTION

In a standard interpretation, the Casimir effect refers to the existence of the attractive force between neutral macroscopic objects due to the fluctuations of the electromagnetic field in the vacuum state. It was originally predicted for the system consisting of two ideally conducting or reflecting plates in vacuum [1] and later on demonstrated also for systems consisting of thick (semi-infinite) dielectric plates separated by empty space [2]. Although soon after the appearance of these seminal papers the theory of the Casimir effect was extended to systems with the gap between the plates filled by a dielectric [3–6] and recently to arbitrary dielectric multilayers [7,8], in most theoretical and experimental considerations of this effect the space between the interacting objects is assumed empty [9–12]. Thus, for example, it is only very recently that the effect of the filling medium on the Casimir force has been measured [13].

Evidently, every finite layer in a multilayer experiences a pressure (force per unit area on its surfaces) due to the vacuum field fluctuation, which depends on both the properties of the layer and those of the surrounding stacks. Changes caused by this pressure (e.g., change of the layer thickness) can therefore be taken as an (alternative) signature of the Casimir effect. In the case of layered systems growing attention has recently been paid to Lifshitz-type configurations with a metallic slab sandwiched between two media. Thus, for example, when discussing some consequences of the zero-point radiation pressure Imry [14] pointed out a strong dependence of the Casimir force pressing a metallic slab, on the properties of the bounding semi-infinite media. Indeed, owing to the magnitude of their dielectric functions relative to that of the slab in the relevant frequency interval, in this configuration even a negative pressure on the slab is possible, corresponding to the repulsive force between the bounding media [3]. Very recently, Benassi and Calandra

[15] used the Lifshitz formula to calculate the Casimir pressure on a (free-electron) metallic slab and explore its dependence on the properties of the slab as well as on the distance and properties of a nearby (metallic) substrate. Since metallic plates are often met as components in micromechanical (MEMS) and nanomechanical (NEMS) systems [16,17], considerations of the Casimir pressure on a metallic slab under various circumstances are also of obvious technological relevance. Having this in mind, in this work we further explore the effects of surrounding media on the Casimir pressure on a metallic slab with the thickness in the submicron range. As in aforementioned works [14,15], in order to keep the discussion simple we adopt the free-electron (plasma) model for metal that is completely described by the electron-plasma frequency ω_p . The thicknesses and lengths are then conveniently measured in terms of the metal plasma wavelength $\lambda_p = 2\pi c / \omega_p$ and, since $\lambda_p \sim 10^2$ nm for typical metals, we therefore consider metallic layers of thicknesses $d \lesssim \lambda_p$.

Of all electromagnetic modes, a special role in the Casimir effect between metallic plates is played by the surface polaritons (SP) and their nonretarded (quasistatic) counterparts, surface plasmons. Thus, it is well known that the vacuum force between two thick metals at small ($\ll \lambda_p$) distances is (almost) entirely given by the SP contribution [18–20]. Recently, however, it has been realized that SP have a fundamental role in the Casimir effect not only at small but at all separations between the metals [21–24]. This indicates that SP modes might play a similar role in the Casimir pressure on a metallic slab and be responsible for its peculiar behavior (e.g., the change of sign). It is therefore of interest to examine more closely the SP contribution to the Casimir energy and pressure for all relevant slab thickness. In order to calculate these quantities and separately, surface contributions to them, we follow our previous work on a similar subject [25] and use the surface mode summation method

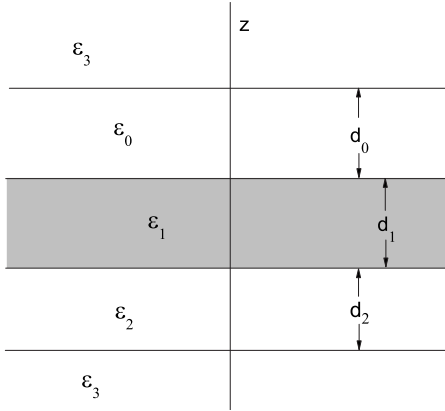


FIG. 1. System considered, schematically.

[6,9,10,12,18,26,27] to derive the Casimir force. This necessarily demands consideration of a lossless system. Since the number of SP modes may be large in the general case of a fully dispersive system leading to a complex analysis, in the discussion we make an additional simplifying approximation, namely, we assume that the dielectric media bounding the metallic slab are described by their static (frequency-independent) permittivities, which involves only two SP modes in the theory. Such an approximation is valid, e.g., for nonpolar dielectrics since for these materials usually $\epsilon(\omega) \simeq \epsilon(0)$ up to frequencies $\sim 10^{15} \text{ s}^{-1}$ [28], and is often made in the theory of the (ordinary) Casimir effect [2–6,9–12]. We shall demonstrate that this approximation can also give good predictions for polar dielectrics, assuming that the characteristic (longitudinal and transverse) frequencies of polar modes in dielectrics are much smaller than ω_p . Although the surface mode method can be applied to any (real) dielectric function, our aim in this paper is to examine and explain general trends using a clearly defined model, rather than to precisely calculate the Casimir pressure in a specific system.

The paper is organized as follows. Resorting to our previous work [25], in Sec. II we briefly derive a Lifshitz-type formula for the Casimir force appropriate for our model and outline a method for separate calculation of the SP contribution to the force. In Sec. III, we discuss the Casimir pressure on a metallic slab between two semi-infinite inert dielectrics and provide an explanation for the change of sign of the Casimir force in the asymmetric configuration. In Sec. IV, we analyze the vacuum pressure on a metallic slab sandwiched between two thin dielectrics and give a simple prescription for changing the pressure in a given direction. Our conclusions are summarized in Sec. V.

II. DESCRIPTION OF THE MODEL

We consider a five layer system consisting of ideally flat dielectric (metallic) plates of thicknesses d_l ($l=0,1,2$) surrounded by an (infinite) dielectric medium 3, as depicted in Fig. 1. All media are assumed lossless and described by (real) dielectric functions $\epsilon_l(\omega)$. Using the same notation as in our previous article [25] (where the mode pattern in such a system is discussed in more detail), we characterize an electromagnetic mode of frequency ω by the wave vector \mathbf{k}

parallel to the system surfaces, the perpendicular wave vector in a layer l , $\beta_l(\omega, k) = [\epsilon_l(\omega)\omega^2/c^2 - k^2]^{1/2}$, and the polarization index $q=p$ or $q=s$, denoting, respectively, the modes with the electric field parallel (TM) or perpendicular (TE) to the plane defined by unit vectors $\hat{\mathbf{k}}$ and $\hat{\mathbf{z}}$. In outer layers, the electric field behaves as $\sim \exp(\pm i\beta_3 z)$ so that propagating (photonic) and evanescent (surface) modes are described by real and imaginary values of β_3 , respectively. In the case of surface modes, the allowed values of β_3 are discrete so we enumerate them by the mode index n .

Adopting the surface mode approach [6,9,10,18,26,27], we define the Casimir energy E_C of the system (with respect to the $l=1$ layer) as

$$E_C = A \int \frac{d^2 \mathbf{k}}{(2\pi)^2} \sum_{q=p,s} \sum_n \frac{\hbar}{2} [\omega_n^q(k, d_1) - \omega_n^q(k, d_1 \rightarrow \infty)], \quad (1)$$

where $\omega_n^q(k, d_1)$ are frequencies of the surface modes and A is the normalization area. The last term here is the standard renormalization term included in order to obtain a finite value for E_C . In the Lifshitz ($\epsilon_1=1$) configuration the force acting on stacks bounding the layer 1 is then given by

$$F_C = - \frac{\partial E_C}{\partial d_1}. \quad (2)$$

Evidently, in the present configuration this force can also be regarded as the force acting on both surfaces of the slab 1, or one can as well consider the pressure on the slab 1, $P_C = (1/A) \partial E_C / \partial d_1$. To be specific, in this work we shall discuss the Casimir force F_C using the above definition, Eq. (2), keeping in mind that the negative (positive) force F_C corresponds to the positive (negative) pressure P_C on the surfaces of the slab and therefore results in squeezing (relaxing) of the slab 1.

As follows from Maxwell's equations, frequencies $\omega_n^q(k)$ are found as solutions of the dispersion relation (obtained from the existence conditions for surface modes)

$$Q^q(\omega, k) \equiv r_-^q(\omega, k) r_+^q(\omega, k) e^{-2\alpha_1 d_1} = 1, \quad (3)$$

where $r_{\pm}^q(\omega, k)$ are reflection coefficients of the upper and lower stack bounding the layer 1 and where, for convenience, we have introduced

$$\alpha_l(\omega, k) = -i\beta_l(\omega, k) = \sqrt{k^2 - \epsilon_l(\omega)\omega^2/c^2}.$$

Note that frequencies $\omega_n^q(k, d_1 \rightarrow \infty)$ are given by the poles of $Q^q(\omega, k)$. Employing the argument theorem and proceeding in the standard way [6,9,10,18,26,27], the sum over the surface modes (n) is converted into an integral over the imaginary frequencies $\xi = -i\omega$. With the substitution $k^2 = (\xi^2/c^2)(p^2 - 1)$, we can put the Casimir energy (1) in the form

$$E_C = \frac{\hbar A}{4\pi^2 c^2} \int_1^\infty dp p \int_0^\infty d\xi \xi^2 \sum_{q=p,s} \ln[1 - Q^q(i\xi, p)], \quad (4)$$

where $Q^q(i\xi, p)$ is obtained from $Q^q(\omega, k)$ by letting $\alpha_l(\omega, k) \rightarrow \alpha_l(i\xi, p) = (\xi/c)\sqrt{p^2 - 1 + \epsilon_l}$, for all layers.

Since the reflection coefficients $r_{\pm}^q(\omega, k)$ in Eq. (3) do not depend on d_1 , we finally arrive at a Lifshitz-type expression for the Casimir force (2) as follows:

$$F_C = -\frac{\hbar A}{2\pi^2 c^2} \int_1^{\infty} dpp \int_0^{\infty} d\xi \xi^2 \alpha_1 \sum_{q=p,s} \frac{Q^q(i\xi, p)}{1 - Q^q(i\xi, p)}. \quad (5)$$

In the following, we use this result to calculate the total Casimir force on the slab $l=1$.

A particularly important contribution to the Casimir energy and force is due to the surface modes which are evanescent in all layers, commonly referred to as surface polaritons (SP). By definition, frequencies of these modes are therefore found as solutions of dispersion relations [Eq. (3)] with all perpendicular wave vectors $\beta_l = i\alpha_l$ being imaginary. As is well known, a dielectric multilayer can support only a finite number of p -polarized SP modes. Accordingly, the SP contribution to the Casimir force, F_C^S , can easily be calculated directly from Eq. (1) as follows:

$$F_C^S = -\frac{\hbar A}{4\pi} \int_0^{\infty} dk k \sum_{\sigma} \frac{\partial \omega_{\sigma}(k)}{\partial d_1}, \quad (6)$$

where σ enumerates solutions of Eq. (3) corresponding to the SP modes. If the contribution from other (photonic) modes, $F_C - F_C^S$, is not significant, one can calculate the Casimir force by taking into account only the contribution from SP modes. Moreover, for systems with a very thin metallic (or dielectric) central layer the retardation of the electromagnetic field can be neglected and one may consider only the nonretarded surface modes, usually referred to as surface plasmons (or phonons). The Casimir force in such systems can be calculated directly from Eq. (6), with frequencies $\omega_{\sigma}(k)$ now being the solutions of the nonretarded dispersion relation as follows:

$$Q^N(\omega, k) \equiv \lim_{c \rightarrow \infty} Q^p(\omega, k) = 1. \quad (7)$$

Evidently, the quantity $Q^N(\omega, k)$ is obtained from $Q^p(\omega, k)$ by letting $\alpha_l \rightarrow k$ for all layers.

III. THIN SLAB BETWEEN TWO SEMI-INFINITE DIELECTRICS

Firstly, we will discuss the force on a metallic slab ($l=1$) bounded by two semi-infinite dielectric media ($l=0, 2$). The slab is described by the dielectric function as follows:

$$\epsilon_1(\omega) = 1 - \frac{\omega_p^2}{\omega^2}, \quad (8)$$

as appropriate for metals with well defined electron-plasma frequency ω_p . We use the plasma wavelength $\lambda_p = 2\pi c/\omega_p$ and $k_p = 2\pi c/\lambda_p$ to scale relevant thicknesses and wave vectors, respectively. The dispersion relation of the surface modes in this system reads [cf. Eq. (3)]

$$Q^q(\omega, k) \equiv r_{01}^q r_{21}^q e^{-2\alpha_1 d_1} = 1, \quad (9)$$

where

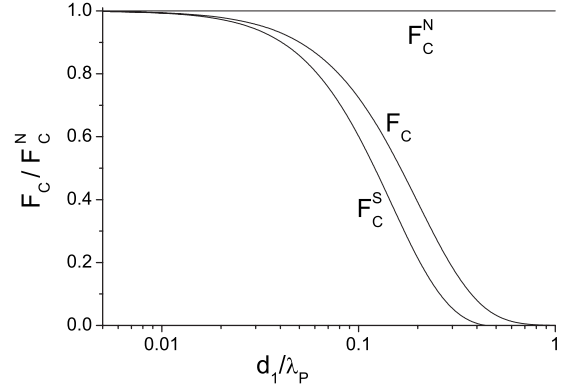


FIG. 2. The total Casimir force F_C compared with the (retarded) SP contribution F_C^S and the (nonretarded) plasmon contribution F_C^N , as a function of a metallic layer thickness d_1 (in units of plasma wavelength λ_p).

$$r_{jl}^p(\omega, k) = \frac{\epsilon_l \alpha_j - \epsilon_j \alpha_l}{\epsilon_l \alpha_j + \epsilon_j \alpha_l}, \quad r_{jl}^s(\omega, k) = \frac{\alpha_j - \alpha_l}{\alpha_j + \alpha_l} \quad (10)$$

are the Fresnel reflection coefficients for the j - l interface. Letting $\alpha_l = k$, in the nonretarded limit we therefore have

$$r_{jl}^N(\omega) \equiv \lim_{c \rightarrow \infty} r_{jl}^p = \frac{\epsilon_l - \epsilon_j}{\epsilon_l + \epsilon_j}, \quad \lim_{c \rightarrow \infty} r_{jl}^s = 0. \quad (11)$$

Let us start with the simplest case of a freestanding ($\epsilon_0 = \epsilon_2 = 1$) metallic slab. Configurations with two “active” surfaces support two SP modes [14]. Their role in the Casimir effect can be most easily understood by considering their nonretarded counterparts whose eigenfrequencies can be given analytically as follows:

$$\omega_{\pm}^2(k) = \frac{\omega_p^2}{2} [1 \pm \exp(-kd_1)].$$

Thus, the integrand in Eq. (6) becomes

$$-k \frac{\partial \omega_{\pm}(k)}{\partial d_1} = \pm \frac{\omega_p^2}{4} \frac{k^2}{\omega_{\pm}(k)} \exp(-kd_1).$$

Obviously, the contribution from the high-frequency (ω_+) mode is positive and from the low-frequency (ω_-) mode is negative leading to the relaxing and pressing component of the Casimir force, respectively. The total (nonretarded) contribution to the force of the two plasmon modes is easily calculated to be pressing

$$F_C^N = -0.0078A \frac{\hbar \omega_p}{d_1^3}, \quad (12)$$

and is a result of the delicate cancellation between the contributions $F_{C-}^N = 7.83F_C^N$ and $F_{C+}^N = -6.83F_C^N$ from the ω_- and ω_+ mode, respectively. This indicates that, with an appropriate selection of surrounding media, the sign of force can be changed, as we shall discuss later. As shown in Fig. 2, F_C^N is a good approximation to the total Casimir force F_C only for very small ($d_1/\lambda_p \lesssim 0.01$) slab thicknesses whereas for thicker slabs the contribution of the (retarded) SP modes F_C^S gives much better approximation. Note also that at d_1/λ_p

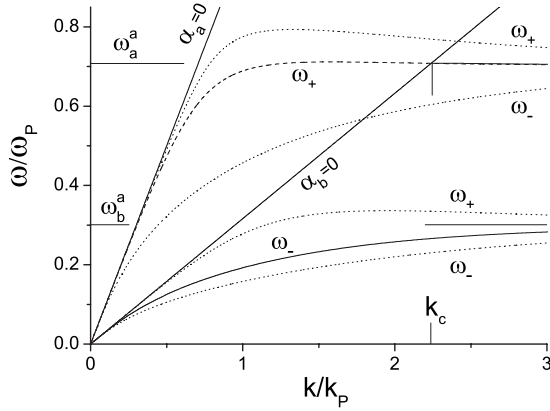


FIG. 3. Dispersion relation $\omega_{\pm}(k)$ of SP modes for a $d=0.1\lambda_p$ thick metallic slab. Dotted lines present SP frequencies in two symmetric configurations: (a) $\epsilon_0=\epsilon_2=1$ and (b) $\epsilon_0=\epsilon_2=10$, with their asymptotic ($k\rightarrow\infty$) values denoted as ω_a^a and ω_b^a , respectively. The corresponding light lines in the surrounding dielectric are denoted as $\alpha_a=0$ and $\alpha_b=0$, respectively. Full lines represent $\omega_{\pm}(k)$ in the asymmetric, $\epsilon_0=1$ and $\epsilon_2=10$ case. Note that in this configuration the ω_+ mode starts with a (cutoff) wave vector $k_c>0$ from the light line $\alpha_b=0$. The dashed line shows the frequency of the ω_+ mode in the configuration with $\epsilon_0=1$ and $|\epsilon_2|=\infty$.

≥ 0.05 the total Casimir force F_C starts to deviate significantly from F_C^N tending to zero much faster than d_1^{-3} .

Let us now discuss the effect of the surrounding media on the Casimir force on the slab. First of all, we will discuss the *symmetric* case with the same dielectric ($\epsilon_0=\epsilon_2$) on both sides of the slab. As follows from Eq. (9) (with $r_{21}^p=r_{01}^p$), the dispersion relations of the corresponding SP modes then read $r_{01}^p e^{-\alpha_1 d_1} = \mp 1$, or alternatively,

$$\frac{\epsilon_1(\omega)}{\epsilon_0} = -\frac{\alpha_1}{\alpha_0} \tanh^{\pm 1}\left(\frac{\alpha_1 d_1}{2}\right), \quad (13)$$

where the upper and lower sign refers to the high-frequency (ω_+) and the low-frequency (ω_-) mode, respectively [29]. In order to simplify the discussion, we consider the surrounding dielectric inert and described by a frequency-independent permittivity. Frequencies $\omega_{\pm}(k)$ of two SP modes existing in this case are shown by dotted lines in Fig. 3 for two different $\epsilon_0=\epsilon_2$ values. Note that frequencies of both SP modes are found below the plasma frequency ω_p as well as below the corresponding light line $\alpha_{a(b)}=0$ (that is, $\omega=kc/\sqrt{\epsilon_{0a(b)}}$) in the external dielectric, and that both frequencies ω_{\pm} tend to the same asymptotic frequency $\omega_{a(b)}^a = \omega_p/\sqrt{1+\epsilon_{0a(b)}}$. Hence, for large values of $\epsilon_0=\epsilon_2$ the contribution from SP modes to the Casimir energy becomes rather small. At the same time, the electromagnetic energy of photonic modes in external dielectric increases with its permittivity so that, for large $\epsilon_0=\epsilon_2$, SP modes no longer give a dominant contribution to the total Casimir energy and force. This is clearly seen in Fig. 4. As before, the SP contribution F_C^S to the Casimir force is the result of cancellation between the (large) positive and negative contributions from ω_+ and ω_- SP modes, respectively. While this cancellation gives the attractive, $F_C^S < 0$ force on a freestanding ($\epsilon_0=1$) slab, for a slab bounded by a dielectric

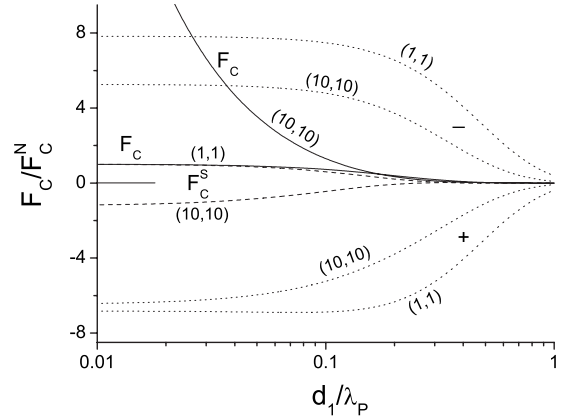


FIG. 4. Casimir force on a metallic slab in the symmetric configuration. The corresponding $\epsilon_0=\epsilon_2$ values are denoted as (ϵ_0, ϵ_2) . Full, dashed, and dotted lines represent the total Casimir force F_C , the contribution to the force of SP modes F_C^S , and the separate contribution of each (+, -) SP mode, respectively.

with a large permittivity we find the repulsive, $F_C^S > 0$ force. Evidently, this is due to the significant change in the dispersion of the SP modes (cf. Fig. 3) resulting in a larger relative contribution of the ω_+ mode to the force. However, the total Casimir force F_C remains attractive due to the much larger “pressing” contribution from the external photonic modes. Accordingly, we can conclude that as the permittivity of the surrounding medium is larger, the Casimir force on the surfaces of the slab is stronger. This trend is particularly evident for thin ($d/\lambda_p < 0.1$) slabs, as seen in Fig. 5.

The Casimir force approaches its maximal value for $|\epsilon_0| \rightarrow \infty$. This case can be realized, e.g., with a metallic external medium having much higher plasma frequency than ω_p —this system obviously closely corresponds to the original Casimir configuration, with a metallic plate instead of an air gap between the perfect mirrors. The Casimir result for the force F_C^0 between two perfect mirrors separated by a vacuum ($\epsilon_1=1$) gap

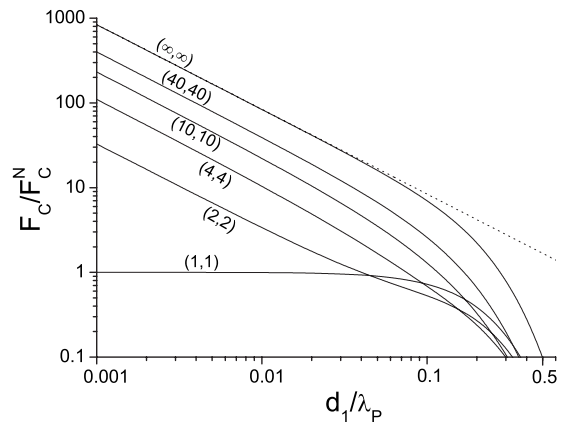


FIG. 5. Casimir force on a symmetrically bounded ($\epsilon_0=\epsilon_2$) metallic slab shown for different dielectric constants of external medium denoted as (ϵ_0, ϵ_2) . The dotted line represents the standard Casimir force F_C^0 , Eq. (14).

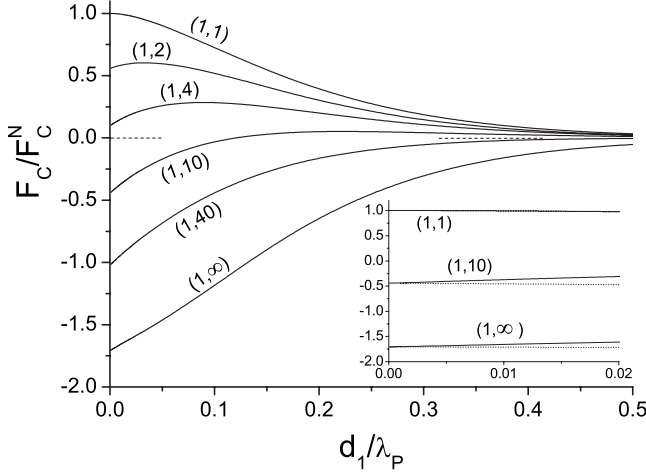


FIG. 6. Casimir force on a metallic slab in the asymmetric configuration. The dielectric constants of surrounding media are denoted as (ϵ_0, ϵ_2) . Inset: Comparison between the total force (full line) and the contributions from SP modes, including the extended part of the (+) SP mode (dotted line). The units correspond to the main figure.

$$F_C^0 = -A \frac{\hbar c \pi^2}{240 d_1^4} \quad (14)$$

is also shown in Fig. 5 for comparison. As seen from this and other curves in Fig. 5, for thin enough ($d_1/\lambda_p < 0.1$) slabs and large permittivity of the external medium, F_C behaves as $\sim 1/d_1^4$ and gradually becomes independent on the properties of the slab. This reflects the fact that for large $|\epsilon_0|$ values the dominant contribution to the force comes from the photonic modes within the slab. Indeed, in the $|\epsilon_0| \rightarrow \infty$ limit, $r_{01}^q = r_{02}^q \rightarrow \delta_{qp} - \delta_{qs}$ in Eq. (9) and the system does not support SP modes anymore but only the modes with frequencies ($\alpha_1 = -in\pi/d_1$)

$$\omega_n^q(k) = \sqrt{\omega_p^2 + c^2(k^2 + n^2\pi^2/d_1^2)}, \quad (15)$$

where n is an integer. In the limit $d_1 \ll \lambda_p$ we can neglect the term ω_p^2 in Eq. (15) so these frequencies, when summed up, lead to the same Casimir energy as in the original Casimir configuration [21], as can also be concluded by comparing (∞, ∞) and F_C^0 curves in Fig. 5.

Let us now consider the Casimir force on boundaries of a thin metallic slab in *asymmetric* configurations, i.e., when the slab is surrounded by two different inert dielectrics ($\epsilon_2 \neq \epsilon_0$). Properties of the total Casimir force in such systems are well known [3,4] so that we only summarize those of them relevant for our analysis. To be specific, we consider the system consisting of a slab supported by a substrate and therefore let $\epsilon_0 = 1$ whereas ϵ_2 is changed. As seen in Fig. 6, with increasing ϵ_2 we obtain a smaller Casimir force on the slab than in the freestanding ($\epsilon_2 = \epsilon_0 = 1$) slab case. For large values of ϵ_2 the Casimir force even changes the sign and the slab relaxes. This first happens at small ($d_1 < 0.1\lambda_p$) slab thicknesses and can therefore be understood by considering the nonretarded (large p) limit of Eq. (5) in conjunction with Eq. (9). With $\alpha_i(i\xi, p) \approx \xi p/c$, we find

$$Q^N(i\xi, p) \approx \frac{[\epsilon_1(i\xi) - 1][\epsilon_1(i\xi) - \epsilon_2]}{[\epsilon_1(i\xi) + 1][\epsilon_1(i\xi) + \epsilon_2]} e^{-2\xi p d_1/c}, \quad (16)$$

so that the force becomes repulsive when $\epsilon_2 > \epsilon_1(i\xi) = 1 + \omega_p^2/\xi^2$ over the relevant frequency range, in accordance with the general condition [3]: $\epsilon_2(i\xi) \geq \epsilon_1(i\xi) \geq \epsilon_0(i\xi)$.

The SP role in this behavior of the Casimir force on the slab surfaces can be explained starting with the $|\epsilon_2| \rightarrow \infty$ case, corresponding to a metallic slab bounded on one side by a perfect mirror. Since the electromagnetic field does not penetrate into medium 2, we have $r_{21}^p = -1$ and the dispersion relation (9) of the SP mode related to the plate-vacuum interface becomes ($r_{01}^p e^{-2\alpha_1 d_1} = -1$)

$$\frac{\epsilon_1(\omega)}{\epsilon_0} = -\frac{\alpha_1}{\alpha_0} \tanh(\alpha_1 d_1). \quad (17)$$

According to Eq. (13), the frequency of this mode is therefore the same as that of the (+) SP mode of the freestanding slab with doubled thickness. For thin slabs (inset in Fig. 6), this SP mode gives the dominant contribution to F_C making the force positive, i.e., relaxing. In the case of finite ϵ_2 , the field penetrates into the medium 2 and from Eq. (9) we find two SP modes [see the full lines in Fig. 3 representing $\omega_{\pm}(k)$ in the (1, 10) configuration]. Since frequencies of these modes must lie below the light line $\alpha_2 = 0$ [$\alpha_b = 0$ in Fig. 3], $\omega_+(k)$ starts at the $\alpha_2 = 0$ light line at some wave vector $k_c > 0$. Accordingly, for large ϵ_2 the cutoff k_c is large and the (positive) contribution of the (+) SP mode to the Casimir force becomes negligible. However, to make a connection with the perfect mirror case (which we expect to be a good approximation for large $|\epsilon_2|$ values) we may “extend” the (+) SP mode into the $\alpha_2^2 < 0$ region in an obvious way: the extended part is calculated with $|\epsilon_2| = \infty$. Indeed, since the cutoff wave vector at $\alpha_2 = 0$ satisfies $r_{21}^p = -1$ regardless of the ϵ_2 value, the (+) SP mode with finite ϵ_2 and the extended (+) SP mode with $|\epsilon_2| = \infty$ meet at the same point at the $\alpha_2 = 0$ light line (Fig. 3), which makes our “extension” procedure consistent [30]. As seen in the inset in Fig. 6, the contribution from so defined SP modes again gives a very good approximation to the total Casimir force at small slab thicknesses. Interestingly enough, this means that for large ϵ_2 the contribution of a continuum of propagating modes from the $\alpha_2^2 < 0$ sector can be replaced by the contribution of only one “extended” SP mode (see further comments on that in the next section). Of course, one may argue that for smaller values of ϵ_2 the extended part of the (+) mode is not a good approximation anymore, but in these cases the space between the $\alpha_0 = 0$ and $\alpha_2 = 0$ lines is very narrow so that the contribution of the (+) mode from this sector does not significantly influence the total Casimir force. Also, in these cases the contribution from the “pressing” (−) SP mode becomes much more important so that by decreasing ϵ_2 the Casimir force will obviously change the sign and become negative.

An issue of great practical importance is the morphological stability of the slab in this type of configuration [31] and we end this section by (roughly) estimating the maximal slab thickness d_1^M compatible with its flat morphology. We note that, by inserting Eq. (16) in Eq. (5), extending the integra-

tion over p to zero and making the substitution $x=2\xi p d_1/c$, the force on a thin slab can be written in a well-known form

$$F_C = -\frac{H}{6\pi d_1^3}, \quad (18)$$

where H is the Hamaker constant given by the corresponding integral. However, instead of calculating this integral for different configurations, we observe that according to Fig. 6 in the thin-slab limit

$$F_C = \eta F_C^N, \quad -1.75 < \eta \leq 1.$$

Accordingly, from Eqs. (12) and (18), the Hamaker constants for these systems lie within the range given by

$$H = 6\pi\eta \times 0.0078\hbar\omega_p, \quad -1.75 < \eta \leq 1. \quad (19)$$

Now, as follows from a simple continuum model, the relaxing Casimir force stabilizes a deposited thin slab upon a critical thickness given by [31]

$$d_1^M = \left(\frac{-HY^2\gamma}{2\pi\sigma^4} \right)^{1/4}, \quad (20)$$

where Y is the Yang modulus of the slab whereas γ and σ are its surface energy and stress, respectively. Taking that for a typical (good) metal $\hbar\omega_p \sim 10$ eV = 1.6×10^{-19} J and [31] $\gamma = 1$ J/m², $Y = 76$ GPa, and $\sigma = 500$ MPa, we find for $\eta = -1$, for example,

$$d_1^M = 7.67 \text{ nm}, \quad d_1^M/\lambda_p = 0.06. \quad (21)$$

Note that this figure is greater than the slab thicknesses considered in Fig. 6 making this estimate consistent. Since the critical slab thickness is system sensitive, for two different configurations a and b , such that $\eta_b = \eta_a + \delta\eta$, we find (assuming negligible change in the mechanical parameters of the slab)

$$\frac{d_{1b}^M}{d_{1a}^M} = \left(\frac{H_b}{H_a} \right)^{1/4} \approx 1 + \frac{\delta\eta}{4\eta_a}, \quad (22)$$

indicating that a small change of the Casimir pressure causes approximately a four times smaller change in the critical thickness of the slab d_1^M . Of course, a more reliable estimate of d_1^M is obtained using the retarded result for the Casimir force and a more realistic description of the system electromagnetic properties [32].

IV. THIN SLAB BETWEEN TWO ARBITRARY THICK DIELECTRICS

Let us now discuss the force on a metallic slab bounded by dielectric layers with finite thicknesses d_0 and d_2 . After some manipulations, we can write the dispersion relations for the surface modes in this system in a similar form as in Eq. (9)

$$Q^{qd} \equiv r_{01}^{qd} r_{21}^{qd} e^{-2\alpha_1 d_1} = 1, \quad (23)$$

where the reflection coefficients r_{l1}^{qd} are given by Eq. (10) with the replacement

$$\alpha_l \rightarrow \alpha_l^{qd} \equiv \alpha_l \frac{(1 - r_{l3}^q e^{-2\alpha_l d_l})}{(1 + r_{l3}^q e^{-2\alpha_l d_l})}, \quad l = 0, 2. \quad (24)$$

Since the coefficients r_{l1}^{qd} obviously do not depend on d_1 , Eq. (5) remains valid and we shall now use it to analyze the influence of finite d_0 and d_2 values on the Casimir force on the layer $l=1$, with respect to dielectric properties of the surrounding medium 3. For a Lifshitz-type configuration, such a discussion was performed in Ref. [25] and the same general conclusions also apply here. Following Ref. [25], in order to obtain a maximum influence of the external medium on F_C , we let $|\epsilon_3| = \infty$, i.e., we consider the Casimir-type configuration with a dielectric-metal-dielectric stack of layers sandwiched between two perfect mirrors. In this case $r_{l3}^p = +1$ and $r_{l3}^s = -1$, so that Eq. (24) gives $\alpha_l^{pd} = \alpha_l \tanh(\alpha_l d_l)$, $\alpha_l^{sd} = \alpha_l / \tanh(\alpha_l d_l)$.

Let us first analyze the modes from the $\alpha_2^2 < 0$ sector of the (ω, k) plane, discussed in the previous section in the $d_1 \rightarrow \infty$ limit. With $\alpha_2 = -i\beta_2$, we find $\alpha_2^{pd} = -\beta_2 \tan(\beta_2 d_2)$ for finite d_2 values. Thus, p -polarized modes that satisfy Eq. (23) are additionally determined by the mode index m ,

$$(2m-1)\frac{\pi}{2d_2} < \beta_2 < (2m+1)\frac{\pi}{2d_2}, \quad m = 0, 1, 2, 3, \dots \quad (25)$$

Note that the $m=0$ mode ($0 \leq \beta_2 < \pi/2d_2$) can be regarded as a continuation of the (+) SP mode in the sector $\alpha_2^2 < 0$ [21,22]. From the requirement (25) we see that for thick ($d_2 \gg \lambda_p$) ϵ_2 layers, the $m=0$ mode approaches the light line $\beta_2=0$, whereas β_2 for $m>0$ modes becomes quasicontinuous. Thus, if we replace in Eq. (23) the oscillatory term $\alpha_2^{pd} \sim \tan(\beta_2 d_2) \rightarrow 0$, we find $r_{21}^{pd} = -1$ and obtain the same equation, Eq. (17), as for the extended (+) SP mode in the configuration with $|\epsilon_2| \rightarrow \infty$. This means that for large d_2 values we may construct the extended mode from pieces of the oscillatory modes, which again justifies our approximation made in the previous section.

Other than by the surrounding medium, the Casimir force on an object can be influenced by the presence of other objects. In order to demonstrate this effect in planar geometry let us now assume that the metallic slab is placed in vacuum ($\epsilon_0 = \epsilon_2 = 1$), that is in an ideal empty planar cavity, and consider the dependence of F_C on its distances d_0 and d_2 from the cavity mirrors.

We first consider the force in the *symmetric* ($d_0 = d_2$) configuration. The results are shown in Fig. 7 with the slab-mirror separation given in the relative units $D_2 = d_2/\lambda_p$. Clearly, the curves $D_2 = \infty$ and $D_2 = 0$ correspond to the curves (1, 1) and (∞, ∞) in Fig. 5, respectively. From the other curves, it is seen that the dependence of F_C on d_2 (loosely) resembles its dependence on ϵ_2 in the case of a slab symmetrically bounded by a semi-infinite dielectric (cf. Fig. 5); as with increasing dielectric function of the surrounding medium (ϵ_2) in the former case, this time the force strongly increases with decreasing cavity distances (d_2). From the inset in Fig. 7, we see that the contribution of SP modes to F_C gradually decreases with decreasing cavity length (d_2) and increasing thickness of the slab (d_1). While the SP contribu-

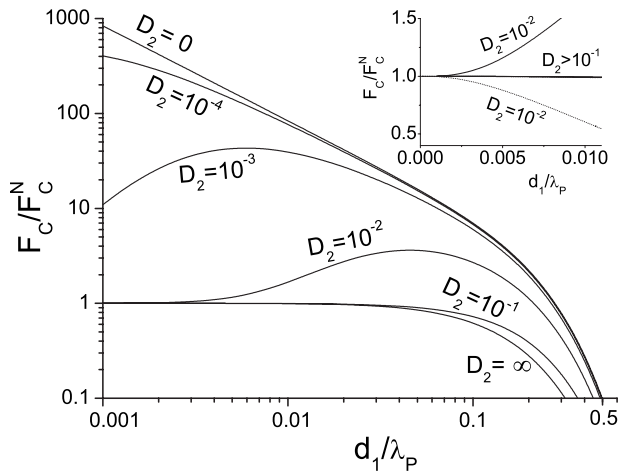


FIG. 7. Casimir force on a thin metallic slab in the center of an empty planar cavity ($\epsilon_0 = \epsilon_2 = 1$) with perfect mirrors. Distances of the slab from the mirrors are denoted by $D_2 = d_2/\lambda_P$. Inset: Comparison between the total force (full line) and the contribution from SP modes (dotted line).

tion from the pressing force can be at most equal to the nonretarded force F_C^N , the contribution from photonic (cavity) modes becomes very large for small cavity lengths [21]. Thus the SP contribution can give reasonable approximation to the total Casimir force only for larger, $d_2 > 0.1\lambda_P$, cavity lengths.

Let us now consider the Casimir force on the slab in the *asymmetric* configuration obtained by letting $d_0 \rightarrow \infty$, which can be regarded as a counterpart of the previously considered system consisting of the metallic slab supported by a dielectric. The dependence of the force on the slab thickness and the mirror-slab distance d_2 is shown in Fig. 8 (see also Ref. [15]). The curves $D_2 = \infty$ and $D_2 = 0$ correspond now to the curves (1, 1) and (1, ∞) in Fig. 6, respectively. By comparing these two figures we see that the d_2 dependence of F_C for

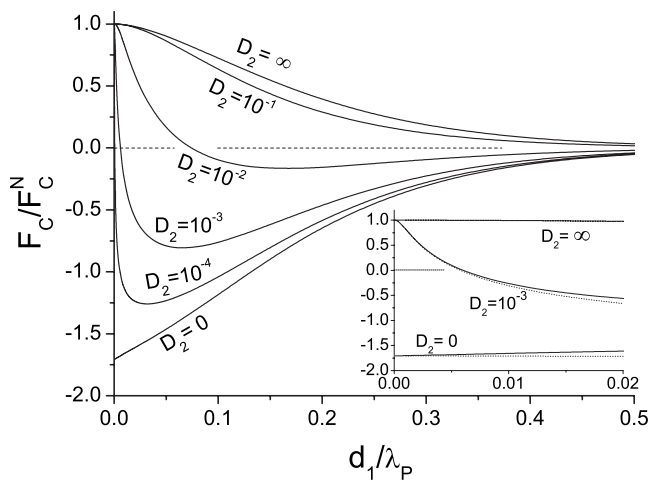


FIG. 8. Casimir force on a metallic slab in front of a perfect mirror. The mirror-slab distance is denoted by $D_2 = d_2/\lambda_P$. Inset: Comparison between the total force (full line) and the contributions from SP modes (dotted line). The units correspond to the main figure.

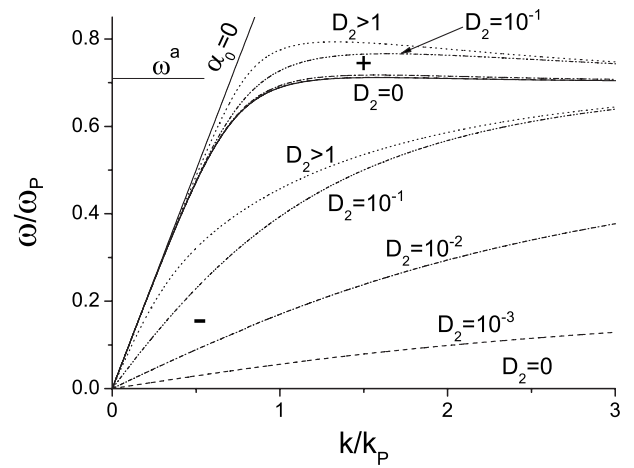


FIG. 9. Dispersion relation $\omega_{\pm}(k)$ of SP modes for a $d_1/\lambda_P = 0.1$ thick metallic slab at a distance $d_2 = D_2\lambda_P$ from a perfect mirror: $D_2 = 0$ (full line), $D_2 = 10^{-3}$ (dashed line), $D_2 = 10^{-2}$ (dash-dotted line), $D_2 = 10^{-1}$ (dash-dotted-dotted line), and $D_2 > 1$ (dotted line).

thicker slabs ($d_1 > 0.1\lambda_P$) again resemble its ϵ_2 dependence in the previously considered system. For thinner slabs, there is a significant change in the behavior of the Casimir force that should be connected with the strong influence of SP modes. This influence is different in the present case as compared with the case shown in Fig. 6. The metallic slab is now surrounded by a vacuum on both sides, so both SP modes are well defined for all wave vectors, as demonstrated in Fig. 9. Notice that the change of d_2 affects the dispersion of (-) much stronger than the (+) SP mode. However, in the $k \rightarrow \infty$ limit (i.e., at wavelengths much smaller than d_2) both modes tend to the same asymptotic frequency $\omega^a = \omega_P/\sqrt{2}$ regardless of the value of d_2 . An obvious exception is the $d_2 = 0$ case, where only the (+) SP mode exists.

The inset in Fig. 8 shows the (expected) dominant contribution of SP modes to the Casimir force for thin slabs so we can understand the behavior of F_C by considering only the properties of SP modes. Thus, in the case of a metallic slab thinner than the mirror-slab distance ($d_1 < d_2$), SP modes give a standard (pressing) contribution to the Casimir force leading to $F_C \approx F_C^N$ in the $d_1 \ll \lambda_P$ limit (see Fig. 2). By decreasing the mirror-slab distance ($d_2 < d_1$), the influence of the “pressing” (-) SP mode becomes less important, so at thin slabs and very thin vacuum layers, the (+) SP mode becomes dominant and the metallic slab relaxes.

Figures 4–8 illustrate the behavior of the Casimir force on a thin metallic slab and the SP contribution to it in a few basic systems for different material (ϵ_0, ϵ_2) and geometrical (d_0, d_2) parameters. Understanding the role of SP modes in building up the Casimir force in these configurations enables one to understand the behavior of the force (and thus to control it) in more complex systems. For example, a typical configuration of practical interest could consist of a metallic slab (1), supported by a dielectric (of permittivity ϵ_0) and separated by a vacuum ($\epsilon_2 = 1$) layer of thickness d_2 from another metallic layer (highly reflecting mirror, $|\epsilon_3| \gg 1$). The Casimir force on the slab in such a system is shown in Fig. 10. As seen, depending on the value of ϵ_0 , one can start with the pressing (relaxing) force on the slab and end up with the

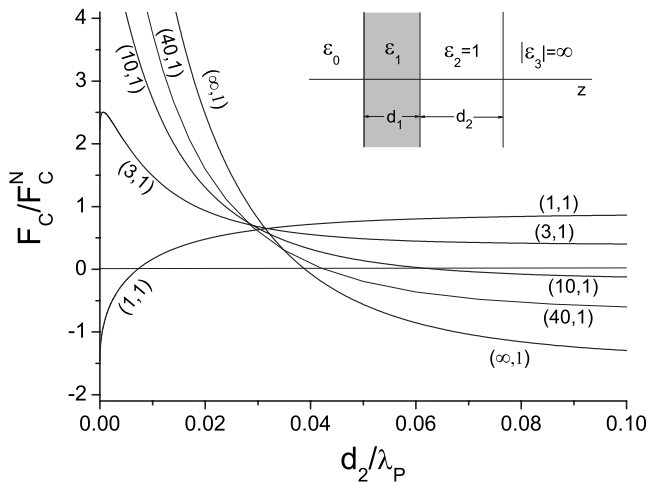


FIG. 10. Casimir force on a $d_1=0.05\lambda_P$ thick metallic slab bounded by a dielectric medium (ϵ_0 , $d_0 \rightarrow \infty$) on one side as a function of the thickness d_2 of a vacuum ($\epsilon_2=1$) layer between the other side of the slab and a perfect mirror (see the inset). The different combinations of dielectric constants are denoted as (ϵ_0, ϵ_2) .

opposite case of the relaxing (pressing) force on the slab simply by tuning properly the mirror-slab distance.

V. SUMMARY

In this paper we have analyzed the Casimir force on surfaces of a thin metallic slab surrounded by dielectric media. This subject is discussed in literature with less detail than the reversed model of a thin dielectric layer surrounded by metallic plates, so our main motivation was to give better insight into the behavior of the Casimir force when the slab is surrounded by media of different dielectric properties. A particularly interesting observation is the change of the Casimir force from squeezing to relaxing, and this effect can be obviously important, e.g., in the design of nanolayers. It turns out that surface polaritons (SP) take a dominant role in such behavior of the Casimir force, so we have taken a simple model in which this effect can be best understood. Accordingly, the slab is described by free-electron dielectric function which depends only on one parameter (electron-plasma frequency ω_p), while the surrounding media are described as inert dielectrics. There are only two SP modes involved in that model, and one of them (ω_+) tries to relax while the other (ω_-) tries to squeeze the slab. The influence on the Casimir force that comes from the propagating (photonic) modes is obviously always squeezing.

Let us briefly comment on the “inert dielectric” approximation employed in this work. In order to estimate, e.g., how the medium dispersion affects our general conclusions, we have performed calculations using for the dielectric functions of surrounding media l ,

$$\epsilon_l(\omega) = \epsilon_{\infty l} \frac{(\omega_{Ll}^2 - \omega^2)}{(\omega_{Tl}^2 - \omega^2)},$$

appropriate to polar dielectrics (ionic crystals) characterized by the longitudinal ω_{Ll} and transverse ω_{Tl} frequencies. By

replacing ϵ_l in our model with the high-frequency permittivity $\epsilon_{\infty l}$, we have obtained (even quantitatively) almost the same results, because the characteristic frequencies (ω_{Ll} , ω_{Tl}) of an ionic crystal are much lower (typically two orders of magnitude) than the plasma frequency ω_p of a metallic slab [33,34]. Of course, for specific materials, one can also analyze the influence of the high-frequency limit ($\epsilon_l \rightarrow 1$), the real (not perfect) screening, the possible losses in all media, etc., but we have found that the general predictions of our approach regarding the influence of the SP modes, remain valid.

An important issue in all these calculations is the scale at which the influence of the Casimir force on a slab can be measured. It is essentially determined by ω_p , so we have scaled all frequencies and distances in the system with ω_p and $\lambda_p = 2\pi c / \omega_p$, respectively, while the force is scaled with the nonretarded value F_C^N [Eq. (12)]. In suitable units, we find $\lambda_p = 1.24 \times 10^3 [\omega_p(\text{eV})]^{-1} \text{ nm}$ and $F_C^N/A = -1.25 \times 10^6 [\omega_p(\text{eV})/d_1(\text{nm})^3] \text{ N/m}^2$. From our calculations, we can infer that $d_c \approx 0.1\lambda_p$ is a critical “thin-slab” thickness below which one can expect a significant change in the behavior of the Casimir force due to the different properties of the surrounding media. In this region ($d_1 \lesssim d_c$), the SP modes have an important role that we have analyzed with respect to the different dielectric as well as geometrical properties of surrounding media. We have pointed out how, by understanding the role of the SP modes, one can achieve, e.g., similar Casimir effect with quite a different setup.

By looking at the electron-plasma frequencies of different materials, i.e., starting from $\omega_p(\text{Cs})=3.3 \text{ eV}$ to $\omega_p(\text{Be})=18.4 \text{ eV}$ [15], we find critical distances in the range $38 \text{ nm} > d_c > 7 \text{ nm}$. Obviously, larger ω_p values will give larger Casimir forces on the surfaces of the metallic slab, but at the same time they will reduce the critical distances (d_c) below which one can expect the strong modification of the Casimir force caused by the external media. At a typical frequency $\omega_p(\text{Na})=6.1 \text{ eV}$ we obtain $d_c=20 \text{ nm}$ so in the thin-slab region, e.g., at $d_1=2 \text{ nm}=0.01\lambda_p$ we find $F_C^N = -0.96 \times 10^6 \text{ N/m}^2$. With such parameters and with the appropriate setup of surrounding media described in the paper, we can obtain an order of magnitude larger Casimir force that tries to squeeze the slab, or at least the same order of magnitude Casimir force that tends to relax the slab. Although such forces will not destroy the slab (because of much stronger cohesion forces among atoms in the slab), it might be possible to observe the changes in the thickness of the slab when implementing different configurations of outer media [14]. The understanding of the behavior and influence of SP modes on the Casimir effect could obviously help in designing specific configuration of thin layers at nanoscale, and could be also used as an assessment of correct interpretation of the Casimir force acting on thin metallic slabs.

ACKNOWLEDGMENT

This work was supported by the Ministry of Science of the Republic of Croatia.

- [1] H. B. G. Casimir, Proc. K. Ned. Akad. Wet. **51**, 793 (1948).
- [2] E. M. Lifshitz, Zh. Eksp. Teor. Fiz. **29**, 94 (1995) [Sov. Phys. JETP **2**, 73 (1956)].
- [3] I. E. Dzyaloshinskii, E. M. Lifshitz, and L. P. Pitaevskii, Adv. Phys. **10**, 165 (1961).
- [4] A. A. Abrikosov, L. P. Gorkov, and I. E. Dzyaloshinski, *Methods of Quantum Field Theory in Statistical Physics* (Prentice-Hall, Englewood Cliffs, NJ, 1963), Chap. 6.
- [5] J. Schwinger, L. L. DeRaad, Jr., and K. A. Milton, Ann. Phys. (N.Y.) **115**, 1 (1978).
- [6] F. Zhou and L. Spruch, Phys. Rev. A **52**, 297 (1995).
- [7] M. S. Tomaš, Phys. Rev. A **66**, 052103 (2002); Phys. Lett. A **342**, 381 (2005).
- [8] C. Raabe, L. Knoll, and D. G. Welsch, Phys. Rev. A **68**, 033810 (2003); C. Raabe and D. G. Welsch, *ibid.* **71**, 013814 (2005).
- [9] P. W. Millonni, *The Quantum Vacuum. An Introduction to Quantum Electrodynamics* (Academic Press, San Diego, 1994).
- [10] M. Bordag, U. Mohiden, and V. M. Mostepanenko, Phys. Rep. **353**, 1 (2001).
- [11] K. A. Milton, J. Phys. A **37**, R209 (2004).
- [12] S. K. Lamoreaux, Rep. Prog. Phys. **68**, 201 (2005).
- [13] J. N. Munday and F. Capasso, Phys. Rev. A **75**, 060102(R) (2007).
- [14] Y. Imry, Phys. Rev. Lett. **95**, 080404 (2005).
- [15] A. Benassi and C. Calandra, J. Phys. A: Math. Theor. **40**, 13453 (2007).
- [16] G. J. Maclay, e-print arXiv:physics/0608196.
- [17] A. Gusso and G. J. Delben, e-print arXiv:0802.2124.
- [18] N. G. van Kampen, B. R. A. Nijboer, and N. K. Schram, Phys. Lett. **26A**, 307 (1968).
- [19] C. Genet, A. Lambrecht, and S. Reynaud, Ann. Fond. Louis Broglie **29**, 331 (2004).
- [20] C. Henkel, K. Joulain, J.-P. Mulet, and J.-J. Greffet, Phys. Rev. A **69**, 023808 (2004).
- [21] F. Intravaia and A. Lambrecht, Phys. Rev. Lett. **94**, 110404 (2005); **96**, 218902 (2006).
- [22] Z. Lenac, Phys. Rev. Lett. **96**, 218901 (2006); F. Intravaia and A. Lambrecht, *ibid.* **96**, 218902 (2006).
- [23] M. Bordag, J. Phys. A **39**, 6173 (2006).
- [24] F. Intravaia, C. Henkel, and A. Lambrecht, Phys. Rev. A **76**, 033820 (2007).
- [25] Z. Lenac and M. S. Tomaš, Phys. Rev. A **75**, 042101 (2007).
- [26] E. Gerlach, Phys. Rev. B **4**, 393 (1971).
- [27] K. Schram, Phys. Lett. **43A**, 282 (1973).
- [28] B. Geyer, G. L. Klimchitskaya, and V. M. Mostepanenko, Ann. Phys. (N.Y.) **323**, 291 (2008).
- [29] The definition of ω_{\pm} modes is not unique: if the symmetry is considered (as, e.g., in Ref. [25]), the symmetric low-frequency mode is usually denoted as ω_{+} and the antisymmetric high-frequency mode as ω_{-} .
- [30] Note that this procedure is quite different from the procedure performed in Ref. [21], where the lowest (TM) propagating mode [a continuation of the (+) SP mode in the $\alpha_0^2 < 0$ sector of the (ω, k) -plane] is denoted as part of the (+) SP mode.
- [31] Z. Suo and Z. Zhang, Phys. Rev. B **58**, 5116 (1998).
- [32] A. Benassi and C. Calandra, J. Phys. A: Math. Theor. **41**, 175401 (2008).
- [33] Z. Lenac, Phys. Rev. A **68**, 063815 (2003).
- [34] M. P. Marder, *Condensed Matter Physics* (John Wiley & Sons, Inc., New York, 2000).